URSI GASS 2020, Rome, Italy, 29 August - 5 September 2020

Capacity Bounds for Backscatter Aided Wireless Transmission on High Speed Rails

Zhongzhao Dou[(1)], Wenjing Zhao[(2)], Renfei Gao[(2)], Suili Feng[(1)], and Gongpu Wang[(2)]
(1) South China University of Technology, China, 510641.
(2) Beijing Jiaotong University, Beijing, China, 100044.

Abstract

In this paper we introduce backscatter technology into wireless communication systems on high speed rails (HSRs). Specifically, we propose a backscatter aided wireless transmission (BAWT) scheme and demonstrate its outperformance over the existing direct wireless transmission (DWT) scheme. We derive the upper and lower bounds of channel capacity for BAWT and prove that the channel capacity for BAWT is larger than that of DWT on certain conditions. Finally, simulation results are provided to corroborate the proposed studies.

1 Introduction

Different from other scenarios of wireless communications, the scenario of high speed rails (HSRs) has the features of high mobility of the transceivers and large penetration loss of the signals passing through train carriages [1] [2].

According to these existing studies, full duplex, relay, beamforming, massive MIMO, or joint estimation and detection are possible candidate technologies to reduce or address the signal penetration loss in wireless communications on HSRs [3]. However, these solutions require complicated signal precessing steps such demodulation and decoding, and meanwhile need expensive radio frequency (RF) components.

In this paper, we introduce another technology, backscatter communication which originated from the second world war [4] and is recently becoming a hot research topic [5] [6], to resolve the signal loss during the transmission between the antennas of base station (BS) and mobile users inside the train. Compared with other existing technologies, utilizing backscatter technology to overcome the signal fading has the advantages of low complexity of signal processing and low cost of circuit implementation. It does not require the signal processing steps of demodulation and decoding, and meanwhile has no need of extra RF components except an amplifier.

In particular, we propose a backscatter aided wireless transmission (BAWT) scheme and compare it with direct wireless transmission (DWT) scheme that is currently used in practical systems on HSRs. We derive the upper and lower bounds of channel capacity for BAWT, and prove that the channel capacity for BAWT is larger than that of DWT on certain conditions.

The rest of the paper is organized as follows. Section 2 introduces DWT and BAWT schemes and the corresponding mathematical system models. Section 3 derives and compares the channel capacities between DWT and BAWT. Section 4 provides simulation results to corroborate the proposed studies and Section 5 summarizes the whole paper.

2 System Model

Suppose that the BS transmits baseband signals $s(t)$ with the carrier frequency f_{cs} and the initial phase θ_s. Assume that the transmission of $s(t)$ follows a general slotted structure in Fig. 2 [7]. Each slot contain N_p training symbols and N_d data symbols, and $N_p + N_d = N$. There is zero padding, i.e., one or several empty symbols, at the end of each slot to avoid interference between slots or different users. We consider two transmission schemes: DWT and BAWT.

2.1 DWT Scheme

The direct wireless channel between the antenna of BS and that of mobile user is $h_0(t)$. In case of DWT, BS transmits straight forward to the mobile user through the channel $h_0(t)$. Thus, the signal received at the antenna of the mobile user inside the train is

$$y_d(t) = h_0(t)s(t)e^{j(2\pi f_{cs}t+\theta_s)} + w_0(t), \tag{1}$$

where $w_0(t)$ denotes the noise at the mobile user.

The receiver will first generate a local carrier signal with carrier frequency f_{cr} and initial phase θ_r, and then multiply it with $y(t)$ to obtain the baseband signal

$$\begin{aligned} r_d(t) =& y_d(t)e^{-j(2\pi f_{cr}t+\theta_r)} \\ =& h_0(t)s(t)e^{j(2\pi\Delta_f t+\Delta_\theta)} + w(t), \end{aligned} \tag{2}$$

where $\Delta_\theta = \theta_s - \theta_r$, $w(t) = w_0(t)e^{-j(2\pi f_{cr}t+\theta_r)}$, and $\Delta_f = f_{cs} - f_{cr}$ is the CFO induced by the crystal oscillators.

Let T_s denote the sampling period. The digital representation of the signal $r_d(t)$ can be obtained as

$$r_d(n) = r_d(t)|_{t=nT_s} = e^{j2\pi\Delta_f n}h(n)s(n) + w(n), \tag{3}$$

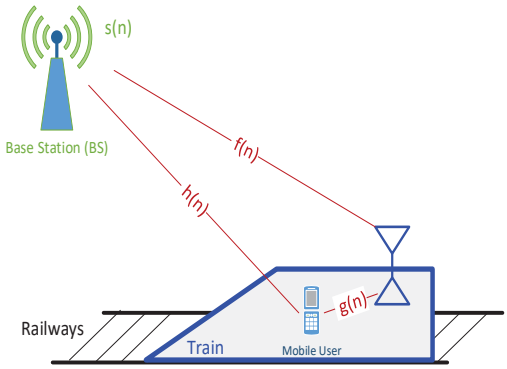

Figure 1. System model.

where $w(n) \sim \mathscr{CN}(0,\sigma_w^2)$ for $n = 1,2,...,N$. Here, $h(n)$ is the combined channel $h(n) = h_0(n)e^{j\Delta_\theta}$.

2.2 BAWT scheme

Suppose the channel between the antenna of the BS and the outside antenna of the train is $f_0(t)$. The signal received at the train antenna is

$$u(t) = f_0(t)s(t)e^{j(2\pi f_{cs}t+\theta_s)}. \tag{4}$$

BAWT scheme requires that the signal $u(t)$ will be delayed for one symbol duration T_s, and then amplified and backscattered by another antenna inside the train. The backscattered signal is

$$b(t) = \alpha\eta u(t-T_s), \tag{5}$$

where α is the amplifying coefficient and η denotes the fading inside the two train antennas.

The mobile user will receive both signals from BS directly and from backscattering

$$y_b(t) = h_0(t)s(t)e^{j(2\pi f_{cs}t+\theta_s)} + g(t)b(t) + w_0(t), \tag{6}$$

where $g(t)$ denotes the channel between mobile user and the inside antenna of the train.

Substituting (4) and (5) into (6) yields

$$\begin{aligned} y_b(t) =& h_0(t)s(t)e^{j(2\pi f_{cs}t+\theta_s)} + w_0(t) \\ &+ \alpha\eta g(t)f_0(t-T_s)s(t-T_s)e^{j(2\pi f_{cs}(t-T_s)+\theta_s)}. \end{aligned} \tag{7}$$

The mobile user will generate a carrier signal to demodulate $y_d(t)$ and will obtain

$$\begin{aligned} r_b(t) =& y_b(t)e^{-j(2\pi f_{cr}t+\theta_r)} \\ =& h_0(t)s(t)e^{j(2\pi\Delta_f t+\Delta_\theta)} + w(t) \\ &+ \alpha\eta g(t)f_0(t-T_s)s(t-T_s)e^{j2\pi\Delta_f t}e^{j\Delta_\theta}e^{-j2\pi f_{cs}T_s}. \end{aligned} \tag{8}$$

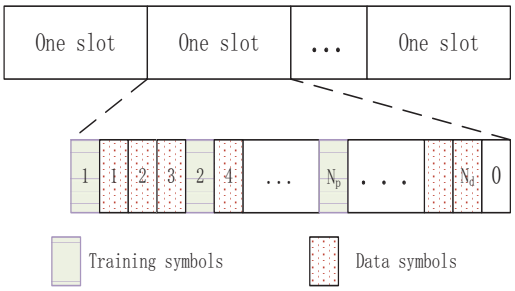

Figure 2. Transmission slot structure.

Noting that the channels $g(t)$ remain almost unchanged during several slots due to limited mobility of the mobile user inside the train. Therefore, it is reasonable to approximate $g(t)$ as a slow-fading variable g_0 within one slot. We assume $g_0 \sim \mathscr{CN}(0,\sigma_{g0}^2)$.

The digital representation of the signal $r_b(t)$ can be obtained as

$$\begin{aligned} & r_b(n) = r_b(t)|_{t=nT_s} \\ =& e^{j2\pi n\Delta_f}h(n)s(n) + e^{j2\pi n\Delta_f}f(n-1)s(n-1) + w(n), \end{aligned} \tag{9}$$

where $f(n-1)$ denotes the combined channel $f(n-1) = \alpha\eta g_0 f_0(n-1)e^{-j2\pi f_{cs}T_s}e^{j\Delta_\theta}$.

3 Capacity Analysis

For brevity of our analysis, let us define the transmitted signals $s(n)$, the channels $h(n)$ and $f(n)$, the received signals $r_d(n)$, and the noise $w(n)$ in one slot as the following vectors $\mathbf{s} = [s(1),s(2),\cdots,s(N)]^T$, $\mathbf{f} = [f(1),h(2),\cdots,f(N)]^T$, $\mathbf{r}_d = [r_d(1),r_d(2),\cdots,r_d(N)]^T$, $\mathbf{w} = [w(1),w(2),\cdots,w(N)]^T$, respectively.

3.1 DWT

We can rewrite (3) as

$$\mathbf{r}_d = \mathbf{D}(\Delta_f)\mathbf{H}\mathbf{s} + \mathbf{w}, \tag{10}$$

where $\mathbf{D}(\Delta_f) = \mathrm{diag}\{e^{j2\pi\Delta_f}, e^{j4\pi\Delta_f},\cdots,e^{j2\pi N\Delta_f}\}$, and $\mathbf{H} = \mathrm{diag}\{h(1),h(2),\cdots,h(N)\}$.

The capacity of (10) is equal to

$$C_{\mathrm{DWT}} = \frac{1}{N}\mathrm{E}\left\{\log\det(\mathbf{I}+\gamma\mathbf{D}(\Delta_\mathrm{f})\mathbf{H}\mathbf{H}^\mathrm{H}\mathbf{D}^\mathrm{H}(\Delta_\mathrm{f}))\right\} \tag{11}$$

$$= \frac{1}{N}\sum_{n=1}^{N}\mathrm{E}\left\{\log(1+\gamma|\mathrm{h(n)}|^2)\right\}, \tag{12}$$

where γ stands for singal-to-noise ratio (SNR).

In the case of $h(n) \sim \mathscr{CN}(0,\sigma_h^2)$, the probability density function of $|h(n)|^2$ is $f_{h^2}(x) = \frac{1}{\sigma_h^2}\exp\left(-\frac{x}{\sigma_h^2}\right)$. Then, with the aid of [8, eq. (4.337)], (12) can be derived as

$$C_{\mathrm{DWT}} = -\exp\left(\frac{1}{\gamma\sigma_h^2}\right)\mathrm{Ei}\left(-\frac{1}{\gamma\sigma_h^2}\right), \tag{13}$$

where $\mathrm{Ei}(x)=\int_{-\infty}^{x}\frac{e^t}{t}dt$ is the exponential integral function [8, eq. (8.211.1)].

3.2 BAWT

Define

$$\mathbf{F}=\mathrm{diag}\{f(1),f(2),\cdots,f(N)\}, \tag{14}$$

$$\bar{\mathbf{r}}_b=[r_b(1),r_b(2),\cdots,r_b(N),r_b(N+1)]^T, \tag{15}$$

$$\bar{\mathbf{w}}=[w(1),w(2),\cdots,w(N),w(N+1)]^T, \tag{16}$$

$$\bar{\mathbf{D}}(\Delta_f)=\mathrm{diag}\{e^{j2\pi\Delta_f},e^{j4\pi\Delta_f},\cdots,e^{j2\pi(N+1)\Delta_f}\}. \tag{17}$$

We can rewrite (9) as

$$\bar{\mathbf{r}}_b=\bar{\mathbf{D}}(\Delta_f)\mathbf{H}_l\mathbf{s}+\bar{\mathbf{D}}(\Delta_f)\mathbf{F}_u\mathbf{s}+\bar{\mathbf{w}}, \tag{18}$$

where

$$\mathbf{H}_l=\begin{bmatrix}\mathbf{H}\\ \mathbf{0}_{N,1}^T\end{bmatrix},\quad \mathbf{F}_u=\begin{bmatrix}\mathbf{0}_{N,1}^T\\ \mathbf{F}\end{bmatrix}, \tag{19}$$

and $\mathbf{0}_{N,1}$ is a vector with N zero elements. Subsequently, we can have

$$\bar{\mathbf{r}}_d=\bar{\mathbf{D}}(\Delta_f)(\mathbf{H}_l+\mathbf{F}_u)\mathbf{s}+\bar{\mathbf{w}}. \tag{20}$$

With CSI at the receiver side, the capacity of (20) is

$$C_{\mathrm{BAWT}}=\frac{1}{N+1}E\{\log\det(\mathbf{I}+\gamma(\mathbf{H}_l+\mathbf{F}_u)(\mathbf{H}_l+\mathbf{F}_u)^H)\}. \tag{21}$$

3.2.1 Lower and Upper Capacity Bounds

It can be readily checked that

$$\begin{aligned}&E\{\log|\mathbf{I}+\gamma\boldsymbol{\Xi}\boldsymbol{\Xi}^H|\}\\ \overset{(a)}{\le}&E\{\log(1+\gamma h^2(1))\}+E\{\log(1+\gamma f^2(N))\}\\ &+\sum_{n=2}^{N}E\{\log(1+\gamma h^2(n)+\gamma f^2(n-1))\}\\ \overset{(b)}{\le}&E\{\log(1+\gamma h^2(1))\}+E\{\log(1+\gamma f^2(N))\}\\ &+\sum_{n=2}^{N}\log(1+\gamma E\{h^2(n)+f^2(n-1)\}),\end{aligned} \tag{22}$$

where (a) and (b) follow by Fischer's inequality and Jensen's inequality, respectively. Suppose the upper bound (22) is denoted by $C_{\mathrm{BAWT}}^{\mathrm{up}'}$, which can be computed as

$$\begin{aligned}C_{\mathrm{BAWT}}^{\mathrm{up}'}=&(N-1)\log(1+\gamma\sigma_h^2+\gamma\sigma_f^2)-\exp\left(\frac{1}{\gamma\sigma_h^2}\right)\times\\ &\mathrm{Ei}\left(-\frac{1}{\gamma\sigma_h^2}\right)-\exp\left(\frac{1}{\gamma\sigma_f^2}\right)\mathrm{Ei}\left(-\frac{1}{\gamma\sigma_f^2}\right).\end{aligned} \tag{23}$$

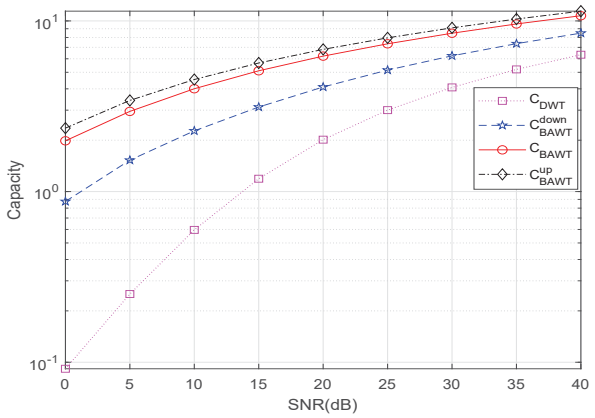

Figure 3. Capacity versus SNR.

Define $\boldsymbol{M}_D$ and $\boldsymbol{M}_U$ as (24) and (25), shown at the top of next page. We can further find

$$\begin{aligned}E\{\log\det(\boldsymbol{M}_D+\boldsymbol{M}_U)\}\ge&E\{\log(\det(\boldsymbol{M}_D)+\det(\boldsymbol{M}_U))\}\\ \ge&E\left\{\log\left(2\sqrt{\det(\boldsymbol{M}_D)\det(\boldsymbol{M}_U)}\right)\right\}.\end{aligned} \tag{26}$$

Denote the lower bound (26) by $C_{\mathrm{BAWT}}^{\mathrm{low}'}$. Then, with the help of [8, eq. (4.331.1)], eq. (26) can be further calculated as

$$\begin{aligned}C_{\mathrm{BAWT}}^{\mathrm{low}'}=&\frac{1}{2}\log(\sigma_h^2)+\frac{N}{2}\log(\sigma_f^2)+\frac{N+1}{2}\big(\log(\gamma)-C\big)\\ &+\log(2)-\frac{N-1}{2}\exp\left(\frac{1}{\gamma\sigma_h^2}\right)\mathrm{Ei}\left(-\frac{1}{\gamma\sigma_h^2}\right).\end{aligned} \tag{27}$$

Denote the upper bound and lower bound of C_{BAWT} (21) by $C_{\mathrm{BAWT}}^{\mathrm{up}}$ and $C_{\mathrm{BAWT}}^{\mathrm{low}}$, respectively. We can obtain

$$\begin{aligned}C_{\mathrm{BAWT}}^{\mathrm{up}}=&\frac{1}{N+1}\Bigg[(N-1)\log(1+\gamma\sigma_h^2+\gamma\sigma_f^2))\\ &-\exp\left(\frac{1}{\gamma\sigma_h^2}\right)\mathrm{Ei}\left(-\frac{1}{\gamma\sigma_h^2}\right)-\exp\left(\frac{1}{\gamma\sigma_f^2}\right)\mathrm{Ei}\left(-\frac{1}{\gamma\sigma_f^2}\right)\Bigg],\end{aligned} \tag{28}$$

$$\begin{aligned}C_{\mathrm{BAWT}}^{\mathrm{low}}=&\frac{1}{N+1}\Bigg[\log(2)+\frac{1}{2}\log(\sigma_h^2)+\frac{N+1}{2}\big(\log(\gamma)-C\big)\\ &+\frac{N}{2}\log(\sigma_f^2)-\frac{N-1}{2}\exp\left(\frac{1}{\gamma\sigma_h^2}\right)\mathrm{Ei}\left(-\frac{1}{\gamma\sigma_h^2}\right)\Bigg],\end{aligned} \tag{29}$$

where $C\approx 0.5772$ is Euler's constant [8, eq. (9.73)].

According to (13) and (29), the channel capacity C_{BAWT} under BAWT scheme is always larger than C_{DWT} under DWT scheme when

$$N\ge\max\left\{0,\left\lceil\frac{-3C_1-C_2-\log(4\sigma_h^2)}{C_1+C_2+\log(\sigma_f^2)}\right\rceil\right\}, \tag{30}$$

where $C_1\triangleq\exp\left(\frac{1}{\gamma\sigma_h^2}\right)\mathrm{Ei}\left(-\frac{1}{\gamma\sigma_h^2}\right)$ and $C_2\triangleq\log(\gamma)-C$.

$$\boldsymbol{M}_D = \begin{bmatrix} \gamma|h(1)|^2 & 0 & 0 & \cdots & 0 & 0 & 0 \\ \gamma h^*(1)f(1) & 1+\gamma|h(2)|^2 & 0 & \cdots & 0 & 0 & 0 \\ \vdots & \vdots & \vdots & \ddots & \vdots & \vdots & \vdots \\ 0 & 0 & 0 & \cdots & 0 & 1+\gamma|h(N)|^2 & 0 \\ 0 & 0 & 0 & \cdots & 0 & \gamma h^*(N)f(N) & 1 \end{bmatrix} \tag{24}$$

$$\boldsymbol{M}_U = \begin{bmatrix} 1 & \gamma h(1)f^*(1) & 0 & \cdots & 0 & 0 & 0 \\ 0 & \gamma|f(1)|^2 & 0 & \cdots & 0 & 0 & 0 \\ \vdots & \vdots & \vdots & \ddots & \vdots & \vdots & \vdots \\ 0 & 0 & 0 & \cdots & 0 & \gamma|f(N-1)|^2 & \gamma h(N)f^*(N) \\ 0 & 0 & 0 & \cdots & 0 & 0 & \gamma|f(N)|^2 \end{bmatrix} \tag{25}$$

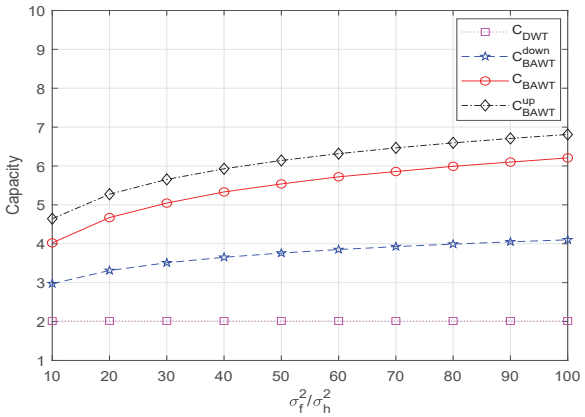

Figure 4. Capacity versus σ_f^2/σ_h^2 when $\gamma = 20dB$.

4 Simulation Results

This section provides numerical examples to evaluate the proposed studies. We set $\sigma_h^2 = 0.1$, $\sigma_f^2 = 10$ and $N = 50$. We assume the channel $f_0(n)$ follows Rician distribution modeled as

$$f_0(n) = \sqrt{\frac{\kappa}{\kappa+1}}\sigma_{f0}e^{j\theta_{f0}} + \sqrt{\frac{1}{\kappa+1}}\mathscr{CN}(0,\sigma_{f0}^2),$$

where κ is the K-factor. Fig. 3 and Fig. 4 illustrate channel capacity versus SNR and the ratio σ_f^2/σ_h^2, respectively. It can be found that the upper bound and lower bound of channel capacity are close to the exact channel capacity. Besides, the BAWT scheme can achieve higher data transmission rate with increasing channel variance σ_f^2 compared with the DWT scheme.

5 Conclusion

In this paper, we introduced backscatter technology into wireless communication systems on HSRs. We compared the capacity performance between BAWT and DWT schemes. To our best knowledge, our work was the first study about backscatter aided wireless communications on HSRs. Many open problems about this topic await further investigation, such as training sequence design, channel encoding, estimation and detection.

References

[1] B. Ai, et al., "Challenges toward wireless communications for high-speed railway," *IEEE Trans. Intelligent Transportation Systems*, vol. 15, no. 5, pp. 2143-2158, Oct. 2014.

[2] R. He, et al., "Propagation channels of 5G millimeter wave vehicle-to-vehicle communications: recent advances and future challenges," to appear in *IEEE Veh. Technol. Magazine*, 2020.

[3] Z. Zhang, X. Chai, K. Long, Athanasios V. Vasilakos and L. Hanzo, "Full-duplex techniques for 5G networks: self-interference cancellation, protocol design and relay selection", *IEEE Commun. Magazine*, vol. 53, no. 5, pp. 128-137, May 2015.

[4] H. Stockman, "Communication by means of reflected power," in *Proc. IRE*, pp.1196-1204, Oct. 1948.

[5] G. Wang, F. Gao, R. Fan, and C. Tellambura, "Ambient backscatter communication systems: detection and performance analysis," *IEEE Trans. Commun.*, vol.64, no.11, pp. 4836-4846, Nov. 2016.

[6] N. Van Huynh, D. T. Hoang, X. Lu, D. Niyato, P. Wang and D. I. Kim, "Ambient backscatter communications: a contemporary survey," *IEEE Commun. Surveys & Tutorials*, vol. 20, no. 4, pp. 2889-2922, Fourth quarter 2018.

[7] M. Dong and L. Tong, "Optimal design and placement of pilot symbols for channel estimation," *IEEE Trans. Signal Process.*, vol. 50, no. 12, pp. 3055-3069, Dec. 2002.

[8] I. S. Gradshteyn and I. M. Ryzhik, *Table of integrals, series and products* , 7th ed. Academic Press Inc, 2007.